Biochemical and Biophysical Research Communications 546 (2021) 178–184

Contents lists available at ScienceDirect

Biochemical and Biophysical Research Communications

journal homepage: www.elsevier.com/locate/ybbrc

APOBEC3B is preferentially expressed at the G2/M phase of cell cycle

Shigeki Hirabayashi [a, b], Kotaro Shirakawa [a], Yoshihito Horisawa [a], Tadahiko Matsumoto [a], Hiroyuki Matsui [a], Hiroyuki Yamazaki [a], Anamaria Daniela Sarca [a], Yasuhiro Kazuma [a], Ryosuke Nomura [a], Yoshinobu Konishi [a], Suguru Takeuchi [a], Emani Stanford [a], Hideya Kawaji [b, c, d], Yasuhiro Murakawa [b, e, f, g], Akifumi Takaori-Kondo [a, *]

[a] Department of Hematology and Oncology, Graduate School of Medicine, Kyoto University, Kyoto, Japan
[b] RIKEN Center for Integrative Medical Sciences, Yokohama, Japan
[c] Tokyo Metropolitan Institute of Medical Sciences, Tokyo, Japan
[d] RIKEN Preventive Medicine and Diagnosis Innovation Program, Wako, Japan
[e] IFOM—the FIRC Institute of Molecular Oncology, Milan, Italy
[f] Department of Medical Systems Genomics, Graduate School of Medicine, Kyoto University, Kyoto, Japan
[g] Institute for Advanced Study of Human Biology (ASHBi), Kyoto University, Kyoto, Japan

ARTICLE INFO

Article history:
Received 6 January 2021
Accepted 2 February 2021
Available online 13 February 2021

Keywords:
APOBEC3B
Single-cell RNA-Sequencing
Multiple myeloma
Normal bone marrow
Cell cycle-dependent
G2/M phase

ABSTRACT

APOBEC3B (A3B) is a cytosine deaminase that converts cytosine to uracil in single-stranded DNA. Cytosine-to-thymine and cytosine-to-guanine base substitution mutations in trinucleotide motifs (APOBEC mutational signatures) were found in various cancers including lymphoid hematological malignancies such as multiple myeloma and A3B has been shown to be an enzymatic source of mutations in those cancers. Although the importance of A3B is being increasingly recognized, it is unclear how A3B expression is regulated in cancer cells as well as normal cells. To answer these fundamental questions, we analyzed 1276 primary myeloma cells using single-cell RNA-sequencing (scRNA-seq) and found that *A3B* was preferentially expressed at the G2/M phase, in sharp contrast to the expression patterns of other APOBEC3 genes. Consistently, we demonstrated that A3B protein was preferentially expressed at the G2/M phase in myeloma cells by cell sorting. We also demonstrated that normal blood cells expressing *A3B* were also enriched in G2/M-phase cells by analyzing scRNA-seq data from 86,493 normal bone marrow mononuclear cells. Furthermore, we revealed that *A3B* was expressed mainly in plasma cells, $CD10^{+}$ B cells and erythroid cells, but not in granulocyte-macrophage progenitors. *A3B* expression profiling in normal blood cells may contribute to understanding the defense mechanism of A3B against viruses, and partially explain the bias of APOBEC mutational signatures in lymphoid but not myeloid malignancies. This study identified the cells and cellular phase in which A3B is highly expressed, which may help reveal the mechanisms behind carcinogenesis and cancer heterogeneity, as well as the biological functions of A3B in normal blood cells.

1. Introduction

Apolipoprotein B mRNA editing enzyme catalytic polypeptide-like 3 (APOBEC3), the genes of which (*APOBEC3A/B/C/D/F/G/H*) are clustered on human chromosome 22, is a cytidine deaminase which converts cytosine to uracil in single-stranded DNA. Recently, cytosine-to-thymine and cytosine-to-guanine base substitution mutations in trinucleotide motifs (TCT/TCG/TCA), namely APOBEC mutational signatures, have been discovered in various cancers such as breast cancer, non-small cell lung cancer, cervical cancer, ovarian cancer, bladder cancer, and hematological malignancies [1–3]. Interestingly, in hematological malignancies, APOBEC-signature mutations represent a high percentage of the total mutations in lymphoid malignancies such as multiple myeloma, lymphoma, acute lymphoid leukemia, but are almost absent in acute

Abbreviations: APOBEC3, A3; single-cell RNA-sequencing, scRNA-seq; bone marrow mononuclear cell, BMMC; Hematopoietic stem cell, HSC; Multipotent progenitor, MPP; Natural killer cell, NK cell; granulocyte-macrophage progenitor, GMP; dendritic cell, DC; Epstein–Barr virus, EBV.

* Corresponding author. Department of Hematology and Oncology, Graduate School of Medicine, Kyoto University, 54 Shogoin Kawahara-cho, Sakyo-ku, Kyoto, 606-8507, Japan.
E-mail address: atakaori@kuhp.kyoto-u.ac.jp (A. Takaori-Kondo).

https://doi.org/10.1016/j.bbrc.2021.02.008

myeloid leukemia [3].

Various evidences showed that, among APOBEC3, *APOBEC3B* (*A3B*) is a key molecular driver of mutagenesis in human cancers [4]. First, *A3B* is overexpressed in multiple primary cancers and cancer cell lines including multiple myeloma [5–8], and high expression of A3B is associated with poor prognosis in multiple myeloma [6], breast cancer [9], non-small cell lung cancer [10] and so on. In addition, upregulation of A3B is correlated with cytosine-to-thymine mutation and overall base-substitution mutation loads in breast cancers [7]. Moreover, we reported that ectopic overexpression of *A3B* in human lymphoma cells induces somatic mutations into the *MYC* locus [5], and that endogenous aberrant expression of *A3B* generates DNA substitutions and deletions in myeloma cells [6]. Overall, the importance of A3B as a source of mutations is being increasingly recognized.

A previous report showed that A3B protein levels were similar in asynchronous cells, cells in S phase and in mitotic phase [11], while other studies showed by using transcriptomic analysis of cancers and normal tissues that *A3B* was co-expressed with the genes associated with cell cycle and cell proliferation [12,13]. Therefore, it is still unclear whether A3B is expressed in a cell cycle-dependent manner. Moreover, it is not fully understood which cells of the human bone marrow express *A3B*. Here, we describe preferential expression of A3B at the G2/M phase in myeloma cells and that *A3B* is expressed mainly in plasma cells, $CD10^{+}$ B cells and erythroid cells using single-cell RNA-sequencing (scRNA-seq) data from multiple myeloma and normal bone marrow samples.

2. Materials and methods

2.1. Clinical sample

All investigations were conducted in accordance with ethical standards and had been approved by the Institutional Review Boards of Kyoto University (G0697). Written informed consent for the banking and subsequent research using their specimens, including genomic and transcriptomic studies, was obtained from the patient. Bone marrow mononuclear cells (BMMCs) were purified from bone marrow aspirates by standard density gradient centrifugation using Lympholyte-H (Cedarlane Laboratories Ltd.) and were cryopreserved in CELLBANKER 1 (Takara Bio Inc.).

2.2. scRNA-seq library preparation and sequencing

Frozen cells from the multiple myeloma patient were resuspended in RPMI-1640 medium with 10% FBS. The cDNA library was constructed from the sample using the Chromium Single Cell 3′ Library & Gel Bead Kit v2 (10x Genomics) according to the manufacturer's instructions. The cDNA library was sequenced on an Illumina HiSeq 2500 platform.

2.3. Processing and analysis of multiple myeloma scRNA-seq data

Alignment to human genome (GRCh38), de-duplication, filtering and generation of gene expression matrixes were performed with the Cell Ranger v3.0.2 (10x Genomics) according to the manufacturer's instructions. The analysis of scRNA-seq data was performed in R version 3.5.1 [14] using the Seurat R package (v3.0.1) [15] based on their instructions. Briefly, cells with a low number of genes (≤200 genes per cell), a high number of genes (≥5000 genes per cell) or a high percentage of mitochondria (≥10% per cell) were excluded. Log-normalization was performed using a size factor of 10,000 molecules for respective cells. For each gene, the variance of gene expression across all cells was calculated and the top 2000 genes with the highest variance were selected and used for principal component analysis. For dimensional reduction, Uniform Manifold Approximation and Projection (UMAP) [16] was utilized with the top 10 principal components and a resolution parameter of 0.8. In this scRNA-seq, only highly expressed genes can be detected. Therefore, when the expression level of *A3B* or *EXO1* per cell was greater than 0, the cell was considered to be *A3B* positive or *EXO1* positive, respectively. To determine the cell cycle phase at single-cell level, cell cycle scores were calculated based on the expression levels of S and G2/M phase markers using Seurat R package (v3.0.1) [15]. The G2/M, S or G1 phase for each cell was determined based on the cell cycle scores.

2.4. Identification of genes co-expressed with A3B and gene ontology enrichment analysis

Spearman's correlation coefficients between *A3B* expression and each gene expression across 1276 myeloma cells were calculated. Gene ontology analysis of positively correlated genes (Spearman's rho ≥ 0.2) was performed using the Database for Annotation, Visualization, and Integrated Discovery (https://david.ncifcrf.gov/home.jsp) [17].

2.5. Cell culture

$AMO1^{A3B-3\times FLAG-IRES-EGFP}$ (AMO1-KI) cells [18] were cultured at 37 °C under 5% CO_2 in RPMI-1640 medium supplemented with 1% Penicillin-Streptomycin-Glutamine (Thermo Fisher Scientific) and 20% FBS.

2.6. Sorting cells by cell cycle phase

1.0×10^6 AMO1-KI cells were incubated at 37 °C under 5% CO_2 for 1 h in complete RPMI-1640 medium containing 5 μM Vybrant DyeCycle Violet Stain (Thermo Fisher Scientific). The cells were analyzed and sorted with BD FACS AriaII (Becton-Dickinson Biosciences). Cell cycle analysis was performed using FlowJo v10 (Becton-Dickinson Biosciences) following the Watson Pragmatic model [19].

2.7. Western blot

Lysates were obtained from AMO1-KI cells sorted by cell cycle phase. Equal amounts of protein were used for SDS-polyacrylamide gel electrophoresis. Proteins were transferred from the gel to Immobilon PVDF membrane (Merck Millipore). After blocking, the membrane was probed with primary antibodies (Monoclonal ANTI-FLAG M2 antibody produced in mouse [1:2000, #F3165, Sigma-Aldrich], Monoclonal Anti-α-Tubulin antibody produced in mouse [1:3000, #T6074, Sigma-Aldrich]) and then probed with secondary antibodies (Anti-Mouse IgG, HRP-Linked Whole Ab Sheep [1:5000, #NA931V, GE Healthcare]). The bands were visualized using Pierce ECL Plus Western Blotting Substrate (Thermo Fisher Scientific) and the signal intensity of the bands was quantified using ImageJ software version 1.51d (https://imagej.nih.gov/ij/).

2.8. G2/M cell cycle arrest experiments

AMO1-KI cells were synchronized by culturing for 24 h at 37 °C under 5% CO_2 in RPMI-1640 medium supplemented with 2 mM thymidine, 1% Penicillin-Streptomycin-Glutamine and 20% FBS. After removing the medium, the cells were washed with 1x D-PBS. Next, the cells were cultured for 2 h in complete RPMI-1640 medium without thymidine and then treated with nocodazole (final concentration of 0.06 μg/ml, Sigma-Aldrich) for 18 h. For cell cycle analysis, G2/M-arrested cells were fixed in cold 70% ethanol for

20 min, and then incubated at 37 °C under 5% CO_2 for 1 h in complete RPMI-1640 medium containing propidium iodide (final concentration of 10 μg/ml, Nacalai) and RNase A (final concentration of 14 units/ml, QIAGEN). Stained cells were analyzed with BD FACS Lyric (Becton-Dickinson Biosciences). Asynchronous cells cultured in complete RPMI-1640 medium without any treatment were used as control.

2.9. Processing and analysis of scRNA-seq data from healthy donors

The preprocessed scRNA-seq data (gene expression matrix) of BMMCs from 20 healthy donors were obtained from GEO: GSE120221 [20]. The authors also used the same kit as us for scRNA-seq library construction and analyzed the data with Cell Ranger v2.0.0 (10x Genomics). The data was analyzed similarly to the analysis as described before but using a resolution parameter of 0.6.

3. Results

3.1. A3B mRNA is preferentially expressed at the G2/M phase

To quantify the genome-wide gene expression at a single-cell level, we performed droplet-based scRNA-seq using BMMCs from a multiple myeloma sample. We analyzed 2081 BMMCs and identified myeloma cells by *SDC1* (CD138), hematopoietic stem cells (HSCs)/multipotent progenitors (MPPs) by *CD34* and *AVP*, $CD4^+$ T cells by *CD3G* and *CD4*, $CD8^+$ T cells by *CD3G* and *CD8A*, classical monocytes by *CD14*, non-classical monocytes by *FCGR3A* (CD16), natural killer (NK) cells by *KLRF1* and *NCAM1* (CD56) and erythroid cells by *HBA1* and *GYPA* (CD235) expression in UMAP projections (Fig. S1, S2 and S3). For further analysis, we focused on myeloma cell populations (Fig. 1A).

We then performed *A3B* expression profiling of the BMMCs and identified *A3B* positive cells mainly among myeloma cells, $CD8^+$ T cells and, unexpectedly, erythroid cells. (Fig. 1B and Fig. S4). Moreover, we found that *A3B* positive cells often co-expressed cell proliferation markers such as *MKI67* and *MCM2* (Fig. S4). To gain a deeper insight into the relationship between *A3B* expression and cell proliferation, we performed cell cycle analysis at a single-cell level, based on transcriptome profiling of each cell (Fig. 1C) [15]. We showed that *A3B* positive myeloma cells were significantly enriched in G2/M-phase cells compared to *A3B* negative myeloma cells (Fig. 1D) and that average expression of *A3B* was the highest in G2/M phase (Fig. 1E). Furthermore, gene ontology enrichment analysis indicated that genes co-expressed with *A3B* (listed in Table S1) were involved in cell division, mitotic nuclear division and sister chromatid cohesion (Fig. 1F).

3.2. Expression levels of A3B protein are higher in G2/M-phase cells than in G1-or S-phase myeloma cells

It is difficult to obtain an A3B specific antibody because of high sequence homology between APOBEC3 proteins. Therefore, we previously generated an A3B reporter myeloma cell line, AMO1-KI, in which FLAG-tag and IRES-EGFP sequences were inserted at the C-

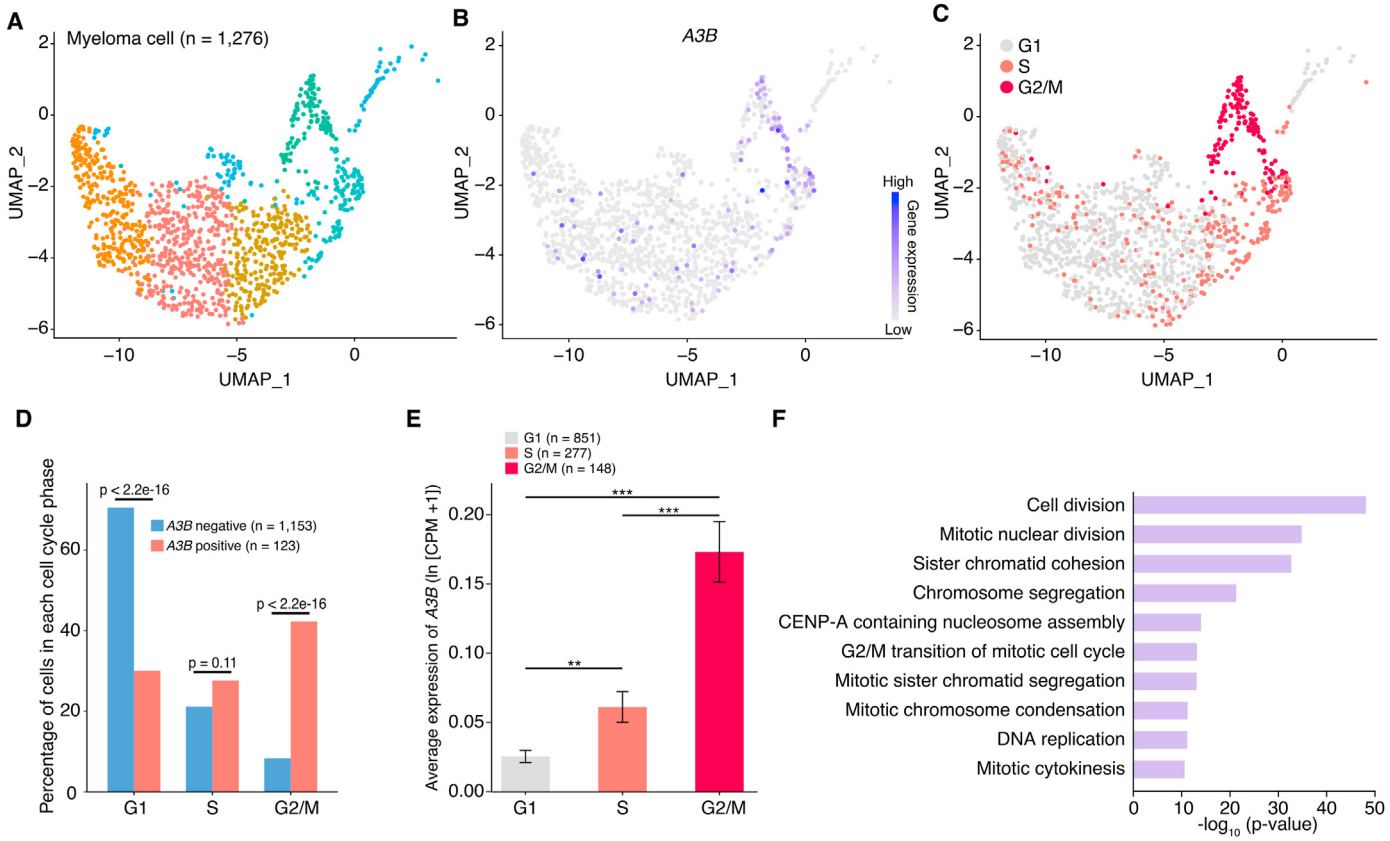

Fig. 1. *APOBEC3B* is preferentially expressed in G2/M-phase myeloma cells. (A) UMAP projection of the myeloma cells surrounded by a red square in Fig. S1. (B) Panel showing the expression level of *APOBEC3B* at single-cell level. (C) Panel showing the cell cycle phase at single-cell level. (D) Percentage of cells in each cell cycle phase among *APOBEC3B* positive and negative myeloma cells. p-value was calculated by two-sided Fisher's exact test. (E) Average expression of *APOBEC3B* in each cell cycle phase. **p < 0.01 and ***p < 0.001 (one-way ANOVA with Tukey's post hoc test). (F) Gene ontology (GO) enrichment analysis of genes co-expressed with *APOBEC3B*. The top 10 GO terms with the lowest p-value are shown. (For interpretation of the references to colour in this figure legend, the reader is referred to the Web version of this article.)

terminal end of the A3B gene [18]. To investigate the expression levels of A3B protein during each cell cycle phase, we performed flow cytometry and sorted cells by cell cycle phase using AMO1-KI cell line. The fluorescence intensity of EGFP in G2/M-phase cells was significantly higher than that in G1-or S-phase cells (Fig. 2A), which indicated that A3B expression was higher in G2/M-phase cells than in G1-or S-phase cells. By performing Western blot analysis of the sorted cells, we confirmed that A3B-FLAG protein was expressed significantly higher in G2/M-phase cells than in G1-or S-phase cells (Fig. 2B). We next treated AMO1-KI cells with

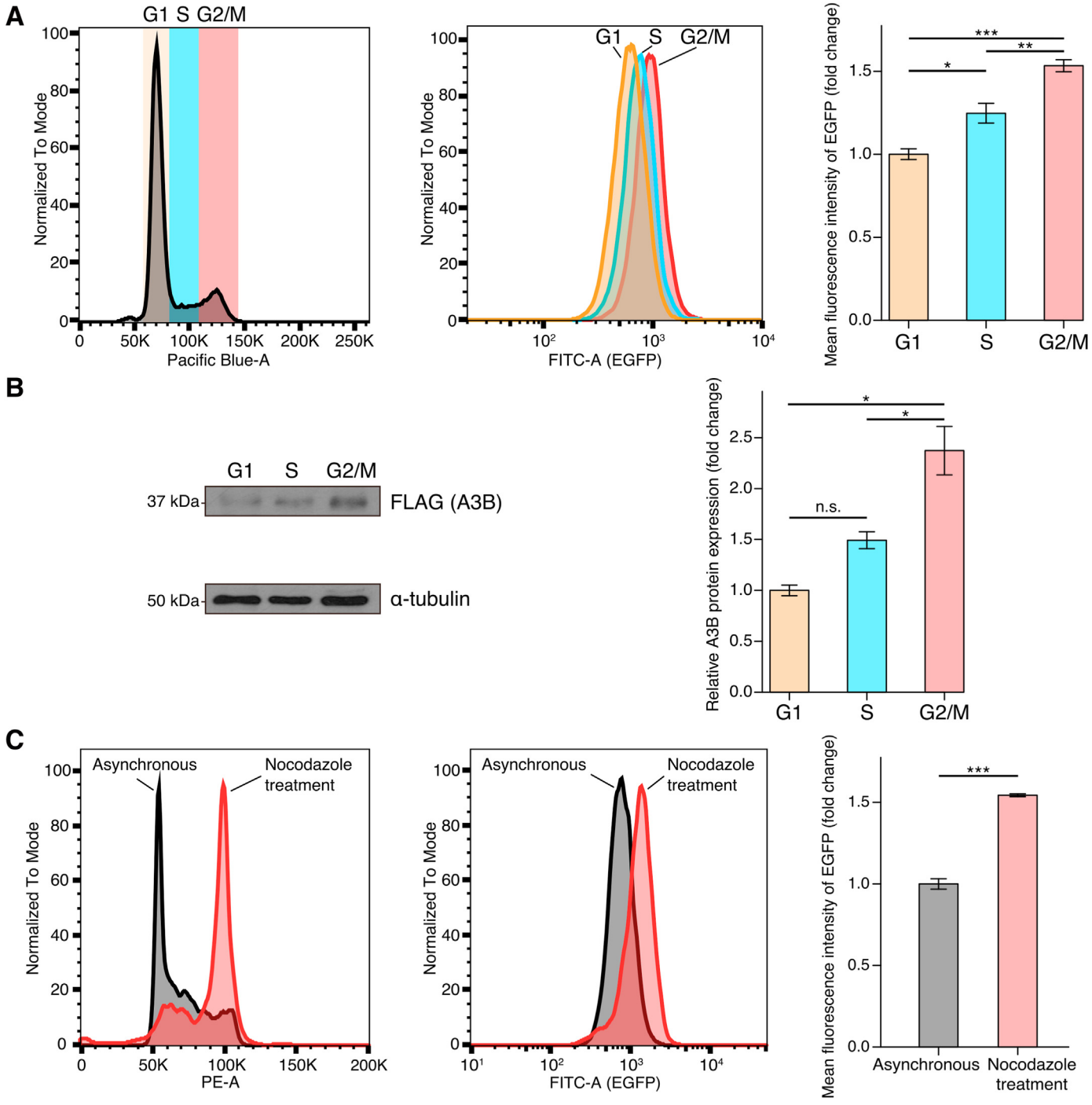

Fig. 2. APOBEC3B protein is highly expressed in G2/M-phase cells. (A) Left panel shows the DNA content of AMO1-KI cells determined by Vybrant DyeCycle Violet Stain. Middle panel shows the level of A3B (EGFP) expression in each cell cycle phase. Right panel shows the mean fluorescence intensity of EGFP relative to that of cells in the G1 phase (n = 3, mean ± sem). *p < 0.05, **p < 0.01 and ***p < 0.001 (one-way ANOVA with Tukey's post hoc test). (B) Western blot analysis of A3B-FLAG in each cell cycle cell fraction. The band signal intensity was quantified by ImageJ and A3B protein expression relative to that in the G1 phase is shown (n = 2, mean ± sem). *p < 0.05 (one-way ANOVA with Tukey's post hoc test). (C) Left panel shows DNA content as determined by propidium iodide staining in asynchronous cells and in cells treated with thymidine and nocodazole which induces G2/M cell cycle arrest. Middle panel shows the level of A3B (EGFP) expression in asynchronous cells and in cells treated with thymidine and nocodazole. Right panel shows mean fluorescence intensity of EGFP relative to that of asynchronous cells (n = 3, mean ± sem). ***p < 0.001 (two-sided Student's t-test). (For interpretation of the references to colour in this figure legend, the reader is referred to the Web version of this article.)

nocodazole which is an inhibitor of microtubule polymerization and causes G2/M cell cycle arrest [21]. First, we confirmed that most of the nocodazole-treated cells were at the G2/M phase using propidium iodide staining and then compared the EGFP fluorescence intensity in nocodazole-treated and asynchronous cells (Fig. 2C). We found that the fluorescence intensity was significantly higher in nocodazole-treated cells compared to asynchronous cells (Fig. 2C), indicating that G2/M-phase cells expressed higher levels of A3B. Overall, these results revealed preferential protein expression of A3B at the G2/M phase in myeloma cells.

3.3. *A3B* is expressed mainly in normal CD10$^+$ B cells, plasma cells and erythroid cells

To perform *A3B* expression profiling of not only tumor cells but also normal bone marrow cells, we obtained scRNA-seq data from 20 healthy donors [20]. We analyzed 86,493 BMMCs and annotated HSCs/MPPs, classical monocytes, non-classical monocytes, CD4$^+$ T cells, CD8$^+$ T cells and NK cells by marker genes as described before. We also identified granulocyte-macrophage progenitors (GMPs) by *IL3RA* (CD123), *FLT3* (CD135) and *CD38*, dendritic cells (DCs) by *ITGAX* (CD11c) and *FCER1A*, plasmacytoid DCs by *CLEC4C* (CD303) and *LILRA4*, CD10$^+$ B cells by *MME* (CD10) and *CD19*, CD20$^+$ B cells by *MS4A1* (CD20), plasma cells by *SDC1* (CD138) and erythroid cells by *HBA1*, *HBD*, *GYPA* (CD235a), *EPOR*, *TFRC*, *GATA1* and *GATA2* expression in UMAP projections (Fig. 3A and Fig. S5, S6 and S7).

By analyzing the cell cycle of normal bone marrow cells, we found that cells expressing *A3B* were significantly enriched in G2/M-phase cells, compared with those not expressing *A3B* (Fig. 3B and C), and that average expression of *A3B* was the highest in G2/M phase (Fig. 3D). Furthermore, we revealed that *A3B* was expressed mainly in CD10$^+$ B cells, plasma cells (including plasma blasts) and, surprisingly, erythroid cells (especially colony-forming unit-erythroids and proerythroblasts) (Fig. 3E). Most of GMPs at the G2/M phase did not express *A3B*, in contrast with CD10$^+$ B cells (Fig. 3B). In each subpopulation, cells expressing *A3B* were also enriched in G2/M-phase cells (Fig. S8A) and average expression of *A3B* was shown in Fig. S8B. We next investigated the expression profiles of all APOBEC3 genes. The other APOBEC3 genes were differently expressed compared to *A3B* in both myeloma cells and normal BMMCs (Fig. 4A and B). In addition, of all APOBEC3 positive cells, cells expressing *A3B* were the most enriched in G2/M-phase cells, both in myeloma cells and in normal BMMCs (Fig. 4C and D). Our data suggest that, unlike other APOBEC3 genes, *A3B* is highly regulated in a cell cycle-dependent manner.

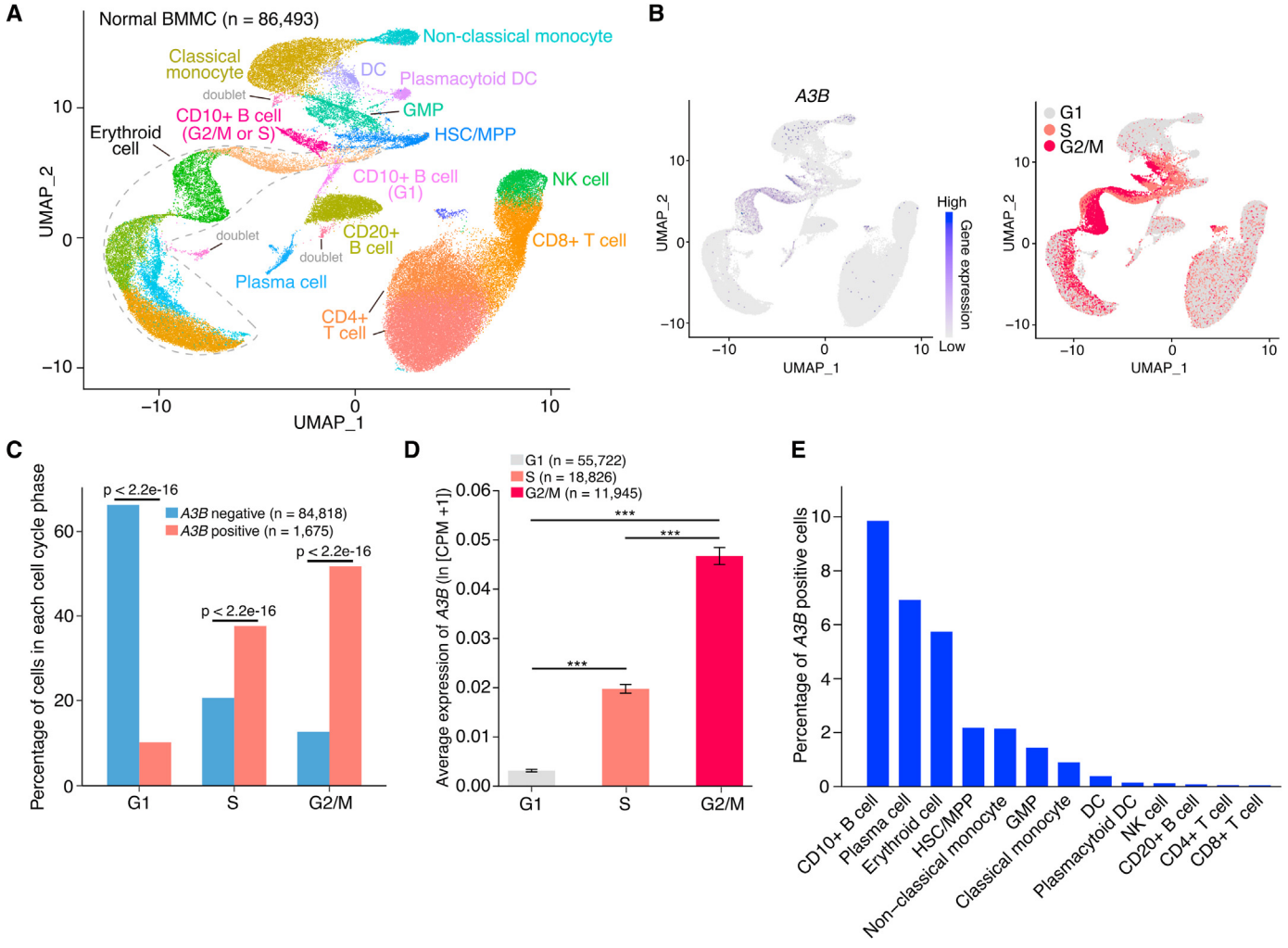

Fig. 3. *APOBEC3B* expression profiling of normal bone marrow cells. (A) UMAP projection of single-cell RNA-sequencing data of bone marrow mononuclear cells from 20 healthy donors. (B) Left panel shows the expression level of *APOBEC3B* at single-cell level. Right panel shows cell cycle phase at single-cell level. (C) Percentage of cells in each cell cycle phase among *APOBEC3B* positive and negative cells. p-value was calculated by two-sided Fisher's exact test. (D) Average expression of *APOBEC3B* in each cell cycle phase. ***p < 0.001 (one-way ANOVA with Tukey's post hoc test). (E) Percentage of *APOBEC3B* positive cells in each cell type. Doublets and an unknown cluster were excluded.

4. Discussion

In this study, we demonstrated at single-cell resolution that *A3B* mRNA is preferentially expressed at the G2/M phase of the cell cycle in both primary myeloma and normal bone marrow cells, in sharp contrast to other APOBEC3 genes. Consistently, we indicated that the protein expression level of A3B is also higher in G2/M phase than in G1 or S phases. To the best of our knowledge, this is the first study to show that both A3B mRNA and protein are preferentially expressed at the G2/M phase.

While previous reports have shown a positive correlation between *A3B* expression and the genes associated with cell proliferation by using bulk RNA-seq in multiple cancers [12,13], our data shows that there is an intratumoral heterogeneity of *A3B* expression, and *A3B* expression is also associated with cell proliferation at a single-cell level. Although APOBEC3 genes have high sequence similarity and are located in close proximity to each other on chromosome 22, *A3B* had a distinct cell cycle dependent expression profile compared to other APOBEC3 genes, suggesting that *A3B* has a different transcriptional regulatory mechanism.

It is important to note the type of mutations caused by APOBEC3. Various types of cancers have APOBEC-signature mutations including hypermutation of small genomic regions, namely 'kataegis' [3]. However, few APOBEC-signature mutations could be explained by kataegis, but were instead explained by unclustered mutations and nonrecurrent diffuse hypermutation, namely 'omikli', identified by Mas-Ponte et al. [22]. They also showed that omikli is associated with DNA mismatch repair, generating single-stranded DNA which APOBEC3 can then easily access. Furthermore, the omikli burden is well correlated with the mRNA expression level of *A3B* and exonuclease 1 (*EXO1*) involved in the DNA mismatch repair pathway [22]. In fact, 44.1% of *EXO1* positive cells expressed *A3B* whereas only 8.7% of *EXO1* negative cells expressed *A3B*, indicating co-expression of *A3B* and *EXO1* at single-cell level (Fig. S9). Moreover, in *in vitro* experiments, knockdown of EXO1 leads to a reduction of mutations induced by A3B [23]. Taken together, A3B and EXO1 might orchestrate the occurrence of A3B-induced mutations.

Aberrant expression of A3B was reported in many cancers [5–8], but the expression profile of *A3B* is not fully described in normal blood cells. Notably, we demonstrated that mainly $CD10^{+}$ B cells, plasma cells, and erythroid cells express *A3B*. Specific cells can express *A3B*, and cells expressing *A3B* have higher proportions of G2/M-phase cells. However, not all types of cells express *A3B* at the G2/M phase. Furthermore, the distinct difference in *A3B* expression between lymphoid cells and GMPs may partially explain why APOBEC mutational signatures are preferentially found in lymphoid malignancies [3].

A3B is known not only as a mutation source, but also as an antiviral enzyme to restrict several viruses. For instance, Cheng et al. demonstrated the antiviral effect of A3B in Epstein-Barr virus (EBV) infection and described an escape mechanism of EBV from A3B [24]. Because EBV plasmid molecules replicate once per cell cycle [25], it seems reasonable that high A3B expression in

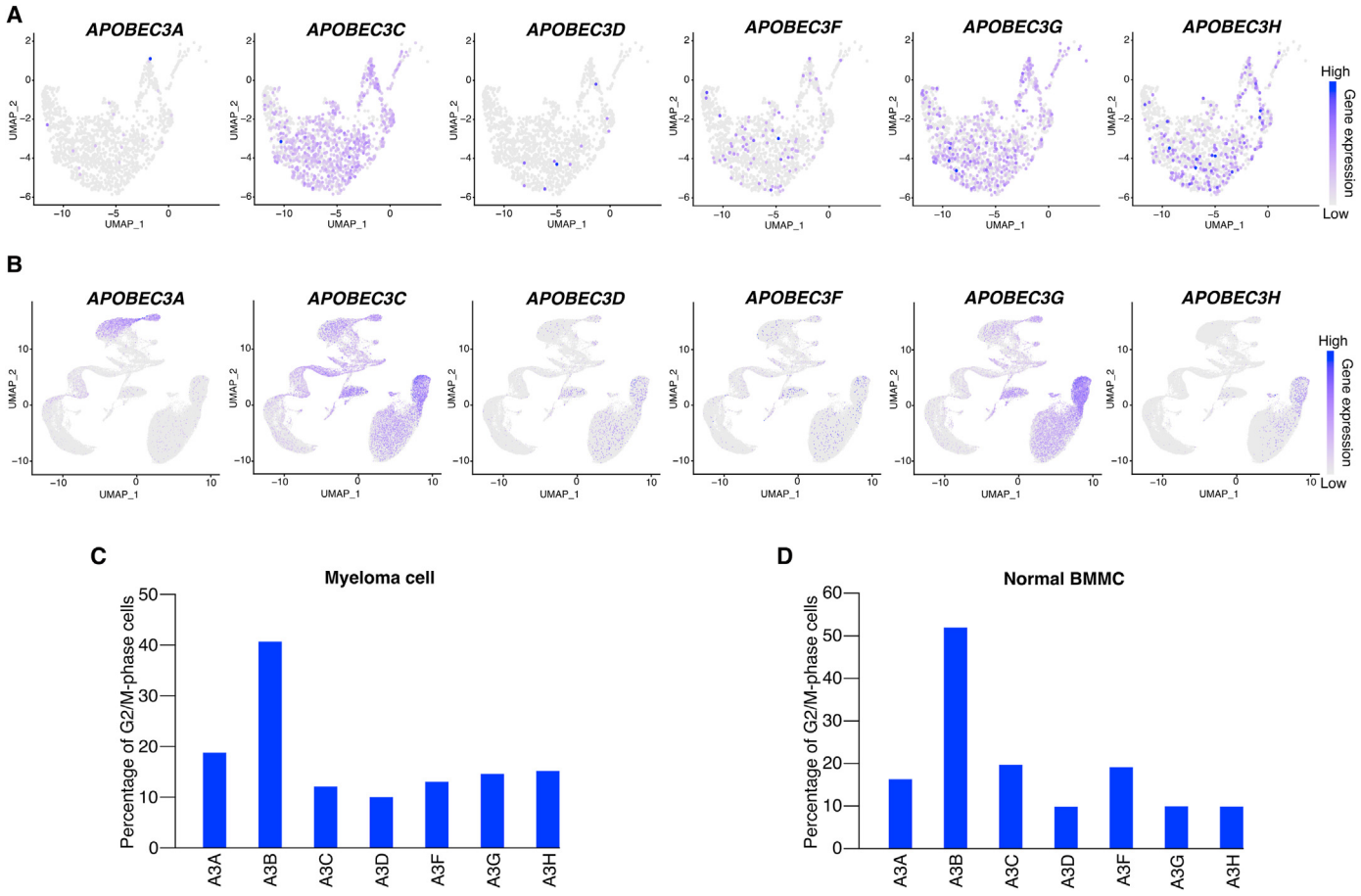

Fig. 4. APOBEC3 genes show different expression patterns. (A–B) UMAP projections showing the expression level of each gene at single-cell resolution in myeloma cells (n = 1276) (A) and normal bone marrow mononuclear cells (n = 86,493) (B). (C–D) Percentage of myeloma cells (n = 1276) (C) and normal bone marrow mononuclear cells (n = 86,493) (D) at the G2/M phase.

proliferating normal B cells could inhibit the active production of the virus. Moreover, a massive APOBEC3 footprint exists in the genome of single-stranded DNA virus parvovirus B19 [26] which infects proerythroblasts [27], replicates in the nuclei [27] and causes G2/M cell cycle arrest [28]. APOBEC3-favored trinucleotide motifs were cleaned from the parvovirus B19 genome sequence, indicating APOBEC3 selection pressure on the virus [26]. A3B may be involved in the APOBEC3 selection pressure on parvovirus B19 because A3B is constitutively nuclear [11] and is highly expressed in G2/M-phase proerythroblasts. Thus, *A3B* expression profiling of normal cells will be useful not only in terms of cancer development, but also in elucidating the antiviral activity of A3B.

In conclusion, we demonstrated that A3B is preferentially expressed at the G2/M phase in both myeloma cells and normal BMMCs, and that mainly $CD10^{+}$ B cells, plasma cells, and erythroid cells express *A3B* in the normal bone marrow. These findings can help reveal the biological functions of A3B and the mechanisms of carcinogenesis and cancer heterogeneity caused by A3B.

Acknowledgements

This work was supported by research grants from the RIKEN Single Cell Project from MEXT to RIKEN Preventive Medicine and Diagnosis Innovation Program, MEXT to RIKEN Center for Integrative Medical Sciences to H.K., by JSPS KAKENHI grant numbers, JP19H03502 to A.T-K., JP18H03992 to Y.M., and RIKEN Junior Research Associate Program to S.H. Computations were partially performed on the NIG supercomputer at ROIS National Institute of Genetics. We would like to thank Mr. Kouno Tsukasa for his support with the library construction.

Appendix A. Supplementary data

Supplementary data to this article can be found online at https://doi.org/10.1016/j.bbrc.2021.02.008.

References

[1] M.B. Burns, N.A. Temiz, R.S. Harris, Evidence for APOBEC3B mutagenesis in multiple human cancers, Nat. Genet. 45 (2013) 977–983, https://doi.org/10.1038/ng.2701.
[2] S.A. Roberts, M.S. Lawrence, L.J. Klimczak, et al., An APOBEC cytidine deaminase mutagenesis pattern is widespread in human cancers, Nat. Genet. 45 (2013) 970–976, https://doi.org/10.1038/ng.2702.
[3] L.B. Alexandrov, S. Nik-Zainal, D.C. Wedge, et al., Signatures of mutational processes in human cancer, Nature 500 (2013) 415–421, https://doi.org/10.1038/nature12477.
[4] J. Zou, C. Wang, X. Ma, et al., APOBEC3B, a molecular driver of mutagenesis in human cancers, Cell Biosci. 7 (2017) 1–7, https://doi.org/10.1186/s13578-017-0156-4.
[5] M. Shinohara, K. Io, K. Shindo, et al., APOBEC3B can impair genomic stability by inducing base substitutions in genomic DNA in human cells, Sci. Rep. 2 (2012) 1–9, https://doi.org/10.1038/srep00806.
[6] H. Yamazaki, K. Shirakawa, T. Matsumoto, et al., Endogenous APOBEC3B overexpression constitutively generates DNA substitutions and deletions in myeloma cells, Sci. Rep. 9 (2019), https://doi.org/10.1038/s41598-019-43575-y.
[7] M.B. Burns, L. Lackey, M.A. Carpenter, et al., APOBEC3B is an enzymatic source of mutation in breast cancer, Nature 494 (2013) 366–370, https://doi.org/10.1038/nature11881.
[8] E.W. Refsland, M.D. Stenglein, K. Shindo, et al., Quantitative profiling of the full APOBEC3 mRNA repertoire in lymphocytes and tissues: implications for HIV-1 restriction, Nucleic Acids Res. 38 (2010) 4274–4284, https://doi.org/10.1093/nar/gkq174.
[9] A.M. Sieuwerts, S. Willis, M.B. Burns, et al., Elevated APOBEC3B correlates with poor outcomes for estrogen-receptor-positive breast cancers, Horm. Cancer. 5 (2014) 405–413, https://doi.org/10.1007/s12672-014-0196-8.
[10] S. Wang, M. Jia, Z. He, X.S. Liu, APOBEC3B and APOBEC mutational signature as potential predictive markers for immunotherapy response in non-small cell lung cancer, Oncogene 37 (2018) 3924–3936, https://doi.org/10.1038/s41388-018-0245-9.
[11] L. Lackey, E.K. Law, W.L. Brown, R.S. Harris, Subcellular localization of the APOBEC3 proteins during mitosis and implications for genomic DNA deamination, Cell Cycle 12 (2013) 762–772, https://doi.org/10.4161/cc.23713.
[12] D.W. Cescon, B. Haibe-Kains, T.W. Mak, APOBEC3B expression in breast cancer reflects cellular proliferation, while a deletion polymorphism is associated with immune activation, Proc. Natl. Acad. Sci. U.S.A. 112 (2015) 2841–2846, https://doi.org/10.1073/pnas.1424869112.
[13] J.C.F. Ng, J. Quist, A. Grigoriadis, et al., Pan-cancer transcriptomic analysis dissects immune and proliferative functions of APOBEC3 cytidine deaminases, Nucleic Acids Res. 47 (2019) 1178–1194, https://doi.org/10.1093/nar/gky1316.
[14] R. Ihaka, R. Gentleman, R: a language for data analysis and graphics, J. Comp. Graph. Stat. 5 (1996) 299–314. Available via, http://www.R-project.org.
[15] T. Stuart, A. Butler, P. Hoffman, et al., Comprehensive integration of single-cell data, Cell 177 (2019) 1888–1902, https://doi.org/10.1016/j.cell.2019.05.031, e21.
[16] E. Becht, L. McInnes, J. Healy, et al., Dimensionality reduction for visualizing single-cell data using UMAP, Nat. Biotechnol. 37 (2019) 38–47, https://doi.org/10.1038/nbt.4314.
[17] D.W. Huang, B.T. Sherman, R.A. Lempicki, Bioinformatics enrichment tools: paths toward the comprehensive functional analysis of large gene lists, Nucleic Acids Res. 37 (2009) 1–13, https://doi.org/10.1093/nar/gkn923.
[18] H. Yamazaki, K. Shirakawa, T. Matsumoto, et al., APOBEC3B reporter myeloma cell lines identify DNA damage response pathways leading to APOBEC3B expression, PloS One 15 (2020) 1–17, https://doi.org/10.1371/journal.pone.0223463.
[19] J.V. Watson, S.H. Chambers, P.J. Smith, A pragmatic approach to the analysis of DNA histograms with a definable G1 peak, Cytometry 8 (1987) 1–8, https://doi.org/10.1002/cyto.990080101.
[20] K.A. Oetjen, K.E. Lindblad, M. Goswami, et al., Human bone marrow assessment by single-cell RNA sequencing, mass cytometry, and flow cytometry, JCI Insight 3 (2018), https://doi.org/10.1172/jci.insight.124928.
[21] G.W. Zieve, D. Turnbull, J.M. Mullins, J.R. McIntosh, Production of large numbers of mitotic mammalian cells by use of the reversible microtubule inhibitor Nocodazole. Nocodazole accumulated mitotic cells, Exp. Cell Res. 126 (1980) 397–405, https://doi.org/10.1016/0014-4827(80)90279-7.
[22] D. Mas-ponte, F. Supek, DNA mismatch repair promotes APOBEC3-mediated diffuse hypermutation in human cancers, Nat. Genet. 52 (2020), https://doi.org/10.1038/s41588-020-0674-6.
[23] B. Shen, J.H. Chapman, M.F. Custance, et al., Perturbation of base excision repair sensitizes breast cancer cells to APOBEC3 deaminase-mediated mutations, Elife 9 (2020) 1–22, https://doi.org/10.7554/eLife.51605.
[24] A.Z. Cheng, J. Yockteng-Melgar, M.C. Jarvis, et al., Epstein–Barr virus BORF2 inhibits cellular APOBEC3B to preserve viral genome integrity, Nat. Microbiol. 4 (2019) 78–88, https://doi.org/10.1038/s41564-018-0284-6.
[25] J.L. Yates, N. Guan, Epstein-Barr virus-derived plasmids replicate only once per cell cycle and are not amplified after entry into cells, J. Virol. 65 (1991) 483–488, https://doi.org/10.1128/JVI.65.1.483-488.1991.
[26] F. Poulain, N. Lejeune, K. Willemart, N.A. Gillet, Footprint of the host restriction factors APOBEC3 on the genome of human viruses, PLoS Pathog. 16 (2020) 1–30, https://doi.org/10.1371/JOURNAL.PPAT.1008718.
[27] P.R. Koduri, Novel cytomorphology of the giant proerythroblasts of parvovirus B19 infection, Am. J. Hematol. 58 (1998) 95–99, https://doi.org/10.1002/(sici)1096-8652, 199806)58:2<95::aid-ajh1>3.0.co;2-v.
[28] E. Morita, K. Tada, H. Chisaka, et al., Human parvovirus B19 induces cell cycle arrest at G2 phase with accumulation of mitotic cyclins, J. Virol. 75 (2001) 7555–7563, https://doi.org/10.1128/jvi.75.16.7555-7563.2001.